GEOPHYSICS, VOL. 78, NO. 4 (JULY-AUGUST 2013); P. E149–E159, 9 FIGS., 4 TABLES.
10.1190/GEO2012-0452.1

Processing and inversion of commercial helicopter time-domain electromagnetic data for environmental assessments and geologic and hydrologic mapping

Joel E. Podgorski[1], Esben Auken[2], Cyril Schamper[2], Anders Vest Christiansen[2], Thomas Kalscheuer[1], and Alan G. Green[1]

ABSTRACT

Helicopter time-domain electromagnetic (HTEM) surveying has historically been used for mineral exploration, but over the past decade it has started to be used in environmental assessments and geologic and hydrologic mapping. Such surveying is a cost-effective means of rapidly acquiring densely spaced data over large regions. At the same time, the quality of HTEM data can suffer from various inaccuracies. We developed an effective strategy for processing and inverting a commercial HTEM data set affected by uncertainties and systematic errors. The delivered data included early time gates contaminated by transmitter currents, noise in late time gates, and amplitude shifts between adjacent flights that appeared as artificial lineations in maps of the data and horizontal slices extracted from inversion models. Multiple processing steps were required to address these issues. Contaminated early time gates and noisy late time gates were semiautomatically identified and eliminated on a record-by-record basis. Timing errors between the transmitter and receiver electronics and inaccuracies in absolute amplitudes were corrected after calibrating selected HTEM data against data simulated from accurate ground-based TEM measurements. After editing and calibration, application of a quasi-3D spatially constrained inversion scheme significantly reduced the artificial lineations. Residual lineations were effectively eliminated after incorporating the transmitter and receiver altitudes and line-to-line amplitude factors in the inversion process. The final inverted model was very different from that generated from the original data provided by the contractor. For example, the average resistivity of the thick surface layer decreased from ~1800 to ~30 Ωm, the depths to the layer boundaries were reduced by 15%–23%, and the artificial lineations were practically eliminated. Our processing and inversion strategy is entirely general, such that with minor system-specific modifications it could be applied to any HTEM data set, including those recorded many years ago.

INTRODUCTION

Electromagnetic (EM) methods enable the resistivity of the subsurface to be investigated via EM induction, thereby avoiding the need for sensors to be in direct contact with the ground. Ground-based EM surveys provide higher resolution information than airborne EM surveys, but the latter provide the possibility to collect large amounts of data across extensive areas in a rapid and cost-effective manner. Although airborne EM methods were originally developed for mineral exploration (Palacky and West, 1991), recent technological advancements have allowed more subtle resistivity variations to be observed than those caused by typical shallow ore deposits. This has led to the diversification of airborne EM applications to include environmental assessments and geologic and hydrologic mapping (Beamish, 2005; Auken et al., 2006, 2009; Best et al., 2006; Eberle and Siemon, 2006; Siemon et al., 2007, 2009; Beamish and Young, 2009; Christiansen et al., 2009; Steuer et al., 2009; Kirkegaard et al., 2011; Siemon et al., 2011; Jørgensen et al., 2012).

During the early years of mineral exploration, the output of airborne EM surveys was used to identify anomalies that could signify the locations of metallic ore deposits (Palacky and West, 1991).

Manuscript received by the Editor 26 October 2012; revised manuscript received 14 February 2013; published online 3 June 2013.
[1]ETH Zurich, Institute of Geophysics, Zurich, Switzerland. E-mail: joel.podgorski@erdw.ethz.ch; thomas@aug.ig.erdw.ethz.ch; green@aug.ig.erdw.ethz.ch.
[2]Aarhus University, Department of Geoscience, Aarhus, Denmark. E-mail: esben.auken@geo.au.dk; cyrilschamper@hotmail.com; anders.vest@geo.au.dk.

The introduction of semiquantitative to quantitative methods (see reviews by Beamish, 2002 and Sattel, 2005) allows depth information to be extracted from airborne EM data. Whereas semiquantitative methods are usually sufficient for the interpretation of the generally high-amplitude anomalies recorded across relatively shallow metallic ores, accurate quantitative methods applied to high-quality low-contrast data are required for dependable inversions and meaningful environmental, geologic, and hydrologic interpretations (Christiansen et al., 2009). As a consequence, standard strategies for processing and inverting commercial airborne EM data collected for mineral exploration may not be sufficient for commercial airborne EM data acquired for other purposes.

Airborne EM measurements can be made continuously in the frequency domain (FEM) or during short time periods (time gates) in the time domain (TEM). Airborne FEM methods usually supply higher resolution information in the shallow subsurface than TEM methods, whereas TEM methods generally provide greater depth penetration because of their more powerful transmitter systems and broader bandwidths (Steuer et al., 2009; Christiansen et al., 2011).

In this paper, we are primarily interested in the processing (including editing) and inversion of commercially recorded helicopter time-domain (HTEM) data required to produce reliable resistivity models for environmental assessments, geologic, and hydrologic mapping, and the exploration of metallic ore bodies that yield only weak EM anomalies. Several different HTEM systems are in use today around the world in a variety of applications. Most of these systems share the same basic features and challenges with respect to data processing and inversion. Our example data set was recorded across the Okavango Delta in Botswana (Figure 1) using the popular helicopter-transported versatile time-domain electromagnetic (VTEM) system. The primary objective of the survey was to map comparatively weak three-dimensional resistivity variations associated with the heterogeneous hydrogeologic conditions of the delta. Relatively standard processing and inversion of these low-contrast data by the commercial contractor yielded erroneous resistivity models and images distorted by significant artifacts.

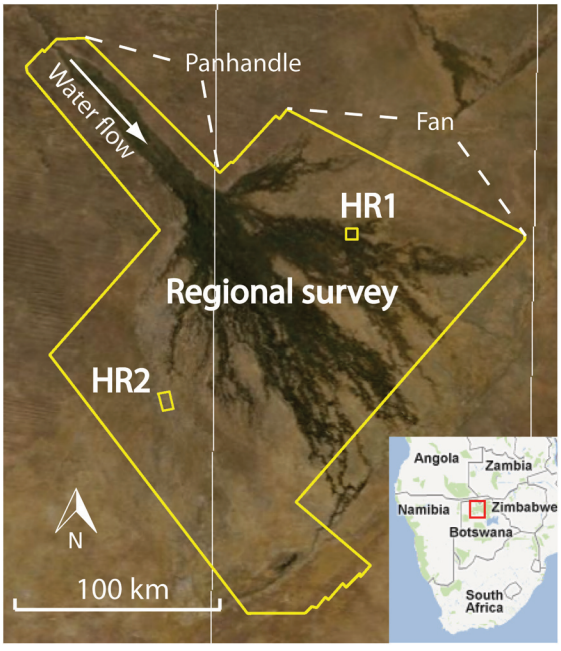

Figure 1. Location of the Okavango Delta and HTEM surveys in northern Botswana. The outer boundary delineates the regional survey (2-km line spacing). Two high-resolution surveys (50-m line spacing) are labeled HR1 and HR2. Inset, location of the main diagram within southern Africa.

After outlining some of the general problems encountered in HTEM and complementary data, we briefly discuss some of the basic modeling and inversion steps. We then introduce the example data set and describe the new processing scheme. Finally, we show the results of applying a pseudo-3D (i.e., spatially constrained) inversion algorithm to the fully processed helicopter data set. Once minor instrument-specific modifications have been made and a few appropriate ground-based TEM data sets have been recorded, our combined processing and inversion strategy could be applied to most other types of HTEM data. In particular, it should be possible to apply this strategy to older HTEM data sets after recording ground-based TEM data at a limited number of locations.

ISSUES ASSOCIATED WITH HTEM SURVEYING

EM techniques are described in most geophysical textbooks, and modern TEM methods are reviewed by Christiansen et al. (2009). Airborne TEM instruments can be used with a helicopter or a fixed-wing aircraft. The instruments can be mounted directly on an aircraft or towed below and behind it. The latter strategy is more common and has the advantage of placing the transmitter and receiver loops some distance from the EM disturbances caused by the aircraft. Helicopter TEM offers the additional advantages of being able to negotiate difficult terrain, fly more slowly allowing for more detailed surveying, and be mobilized with relative ease. As such, this has become a particularly widespread surveying method over the past decade. The most commonly used HTEM systems are AeroTEM, HeliTEM, HoistEM, SkyTEM, and VTEM (Fountain et al., 2005; Christiansen et al., 2009).

General problems that need to be resolved before data inversion

Christiansen et al. (2009, 2011) describe most of the important processes that need to be applied to obtain accurate HTEM data ready for modeling and inversion. These include the following: (1) determining the coordinates and altitudes of each data point using differential GPS and radar/laser altimeter measurements, (2) data leveling, (3) removing data spikes, (4) eliminating poor quality data, including data affected by anthropogenic objects, (5) applying corrections for transmitter current variations and system drift, (6) deleting early time gates contaminated by persistent transmitter currents in the transmitter coil, (7) deleting excessively noisy late time gates, (8) correcting any timing errors between the transmitter and receiver electronics, (9) calibrating data amplitudes, and (10) correcting altitudes.

For contracted commercial surveys, determining the coordinates and altitudes for each data point is relatively routine and data leveling is typically applied by the contractor using proprietary software. Data leveling is based on in-field measurements that provide the necessary information to make first-order corrections for transmitter current variations and instrument drift. Processes 3 and 4 are usually accomplished by applying various filtering techniques and manual editing. For the large EM anomalies typical of relatively shallow metallic ore bodies, semiquantitative to quantitative modeling and

inversion can then be applied to such edited and corrected data. For the much weaker signals associated with environmental assessments, geologic and hydrologic mapping, and the exploration of low-contrast or deep metallic ore bodies, the corrections may need to be improved and processes 6–10 implemented.

Transmitter current variations and system drift

For systems that include complex electronics, large power supplies, and big loops, recordings may be significantly influenced by variations in the transmitter current. In addition, recordings are invariably affected by drift in the transmitter and receiver electronics that result from changes in temperature, humidity, and pressure. Amplitude variations and system drift can cause offsets in data values recorded along adjacent lines. Transmitter current can be monitored and system drift can be estimated from measurements made at high elevations not influenced by the earth. The high-elevation measurements are subtracted from the production data during leveling. In most cases, the contractor applies proprietary algorithms for this purpose.

Primary-field contamination of early times and noisy late times

A finite time is required for the complete extinction of current in the transmitter loop. The earliest time gates will be contaminated if current continues to flow in the transmitter loop while they are being recorded (Figure 2). It is the early time gates that provide information on the shallow subsurface (Nabighian and Macnae, 1991), but including contaminated time gates in the inversion process will result in erroneous resistivity models. Because currents take longer to decay in big loops, this problem is exacerbated with the trend to larger moment systems. On the other hand, the goal of larger moments is to probe more deeply into the earth. Usually, a compromise in moment size is made based on the expected target depths (alternatively, at least one HTEM system has two transmitter moments: a low moment with rapid transmitter current decay for mapping the shallow subsurface and a high moment for investigating deeper structures, Sørensen and Auken, 2004). The challenge is then to eliminate just enough early time gates to avoid the effects of transmitter-current contamination while maintaining a sufficient number to image the shallow subsurface.

As the signal decays, the ambient noise may eventually overwhelm the signal in the late time gates. Flawed resistivity models will be a consequence of including overly noisy late time gates in the inversion process. Again, the challenge is to remove only those time gates that negatively affect the inversion process.

Timing errors between the transmitter and receiver electronics

An associated issue is that the time between current extinction and the first time gate may only be poorly determined (zero-time for a recording is usually defined at either the beginning or the end of the current turn-off ramp). This is a particular problem when using high-moment systems to map shallow features (Christiansen et al., 2011). To resolve this problem, either the instrument needs to be calibrated at a well-understood test site (Foged et al., 2013) or its performance needs to be compared to that of a well-calibrated instrument at the investigation site.

Systematic amplitude effects

Several HTEM systems are calibrated in a relative sense, whereas others are calibrated absolutely in the laboratory or at a test site (Christiansen et al., 2009). To extract reliable quantitative information from data acquired by a relatively calibrated system requires additional absolute calibration at the investigation site, for example, by comparing the data with measurements made using a well-calibrated instrument at the same location.

Inaccurate altimetry

Another common issue with airborne TEM is inaccurate altimetry, which can result in large errors in modeled near-surface resistivity (Davis and Macnae, 2008; Macnae and Baron-Hay, 2010). Airborne systems use either radar or laser altimeters. Radar instruments can overestimate ground clearance by up to 5 m over rugged land, likely due to surface roughness and soil moisture (Brodie and Lane, 2003). Radar and laser systems suffer from the so-called canopy effect, which results from an underestimation of ground clearance due to the presence of trees, bushes, and other vegetation (Beamish, 2002). Furthermore, because the distance between the altimeter mounted directly on the helicopter and the suspended TEM system can vary slightly according to flight speed, wind, and turbulence, the altitudes provided by the contractor based on helicopter-mounted altimetry may contain small but significant errors.

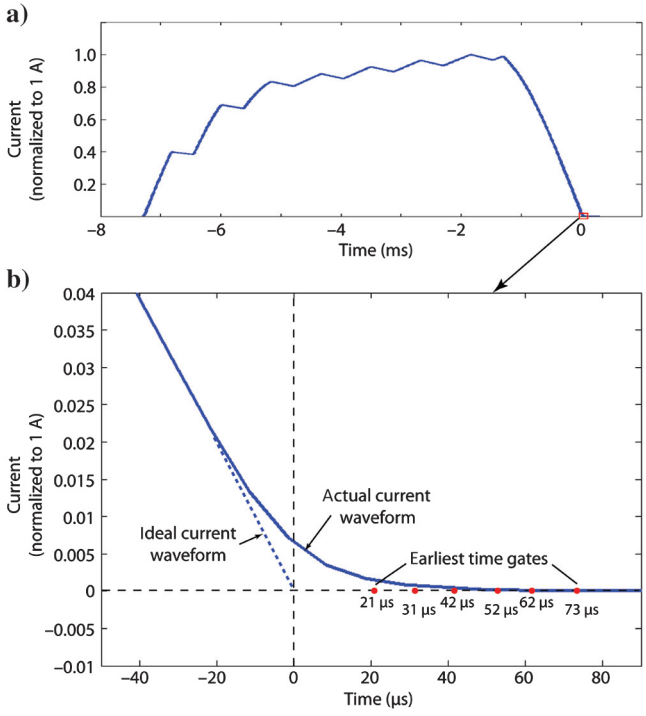

Figure 2. First quarter-period of the VTEM transmitter current waveform, which is positive for 7343 µs before the contractor-defined 0 µs point. (a) Quarter-period of waveform normalized to 1 A. The current waveform begins at 0 A and ends at approximately 0 A. (b) Magnification of the end of the current turn-off ramp shows that the current does not drop to 0 A at the contractor-defined 0 µs point. The first four time gates are recorded while significant current continues to flow in the transmitter loop.

Data presentation, modeling, and inversion

Numerous methods exist for representing airborne TEM data and models with varying degrees of sophistication. The simplest is to plot the recorded data by time gate on a map (Palacky and West, 1991). The displayed format can be either as recorded in dB/dt (V/m^2) or as apparent resistivity ρ_a (Ωm). Somewhat more informative are approximate 2D models of conductivity versus depth provided by conductivity depth transforms (Macnae et al., 1991; Wynn et al., 2005). More advanced are models based on inversion, which involves iteratively deriving depth and resistivity values consistent with the measured data. Inversion of EM data usually involves the concatenation of independent 1D models (see reviews by Beamish, 2002 and Sattel, 2005) or the construction of pseudo-2D and pseudo-3D models from suites of 1D layered models that are constrained to be horizontally smoothly varying, conditions typical of sedimentary environments. The pseudo-2D and pseudo-3D models are based on laterally constrained 1D inversions (Auken and Christiansen, 2004) and spatially constrained 1D inversions (Viezzoli et al., 2008), respectively. Although algorithms for the full 3D inversion of airborne EM data are available (e.g., Brodie and Sambridge, 2006), the size of many airborne EM data sets makes this computationally intractable. However, 3D inversions of large airborne EM data sets have recently been made possible by implementing a moving footprint approach, whereby sequential 3D inversions of small subsets of data yield reliable models at considerably reduced computational costs (Cox et al., 2012; Yang and Oldenburg, 2012).

DATA

Our example data set was acquired during a 2007 VTEM survey of the Okavango Delta, Botswana, the purpose of which was to map the fresh and saline water aquifers of the delta. Three survey areas were flown (Figure 1): a regional survey covering the entire delta with 2-km line spacing and two much smaller high-resolution surveys, HR1 and HR2, with 50-m line spacing. Details on the recording parameters are provided in Table 1. In total, more than 16,000 line-km of data were flown with raw data stacks every ~2.5 m.

The delivered data were subjected to quality control and relatively standard processing by the contractor. These steps included filtering to remove spikes, compensating for current fluctuations using a proprietary algorithm, and leveling to reduce the effect of system drift and bias. The time-dependent leveling factors were based on interpolations between high-altitude measurements made at the beginning and end of each day of flying. The net results of applying these factors were checked by comparing voltage levels recorded on two adjacent flights and correcting obvious errors.

In addition to the processed data, the contractor provided maps of dB/dt and ρ_a for a selection of time gates and various resistivity models obtained from inverting the three data sets using pseudo-2D and pseudo-3D inversion schemes; early versions of the computer codes described by Auken and Christiansen (2004) and Viezzoli et al. (2008) were used for this purpose. Even though time gates up to 52 μs and later were contaminated by persistent transmitter currents (Figure 2b), the principal resistivity models were based on inversions of data contained in the 31–7828 μs time gates. All maps and resultant resistivity models contained linear artifacts parallel to the recording lines that obscured authentic low-contrast features in the data and models. Low-pass spatial filtering by the contractor helped suppress the lineations in the resistivity models for the two high-resolution survey areas. This approach is, however, unsatisfactory in that it is only a visual correction.

Figure 3 shows dB/dt maps of the 99- and 5495-μs time gates from the HR2 survey area. The artificial lineations in these and all other dB/dt maps are consequences of applying inadequate corrections for transmitter current variations, bias, and system drift (note that the lineations would not be so prominent had the maps contained a much larger range of dB/dt values typical of relatively shallow metallic ore deposits within resistive bedrock). It is these small amplitude variations between flight lines that cause the artificial lineations in the contractor's resistivity models. Moreover, any systematic errors in the amplitudes and altitudes could affect the average model resistivities and layer-boundary depths.

Certain key information was not provided by the contractor, including the actual high-altitude measurements, tilt data (very likely not recorded), and details on the preprocessing. After considering the inadequate editing of contaminated early time gates and artificial lineations in the dB/dt maps and resistivity models together with possible transmitter-to-receiver timing errors, possible systematic errors in the recorded amplitudes (the calibration of the VTEM system is relative rather than absolute; Christiansen et al., 2009, 2011), and inevitable minor inaccuracies in the altimetry, it was clear that additional quality control, processing, and inversion were necessary to produce reliable resistivity models from the Okavango Delta HTEM data. In the following, we describe our novel data editing and timing and amplitude calibration procedures and our integrated approach for simultaneously inverting and accounting for system drift and small altimetry errors.

METHODS AND RESULTS

Stacking the data

The original 2.5-m-spaced data were first stacked to improve signal-to-noise ratios and provide data at a 25-m sample interval (Table 1). To take advantage of the naturally broader footprints at greater depths and allow for more noise to be averaged out in later time gates, the width of the stacking window was increased to 250 m for time gates >1000 μs.

Data editing

Inspection of the original data demonstrated the need to edit early and late time gates from most recordings. The first several gates (21–52 μs) generally showed the effects of residual current in the transmitter loop (Figure 2b). In some sections of the survey area, transmitter-current contamination affected only the first couple of gates and in other sections its effects extended up to the 99-μs time gate. Rather than uniformly excluding early gates in all recordings, gates were semiautomatically identified and removed on the basis of slope changes in the dB/dt transients that were indicative of transmitter-current contamination. After inspection of recordings from many locations throughout the survey area, we found that most of the transmitter-current contamination could be eliminated by purging early time gates that exceeded a slope-change threshold of $\pm 0.2\ \ln(\mathrm{dBdt})/\ln(\mathrm{time})$. For each recording, the latest gate affected by transmitter-current contamination and all prior gates were removed (Figures 2 and 4). Table 2 shows the percentage of recordings from the three survey areas for which early time gates were eliminated (21–99 μs). Nearly all of the first four gates

(21–52 μs) were eliminated. Significantly fewer recordings required removal of the following four gates (62–99 μs).

For most regions, the VTEM data were of uniformly high quality due to the high moment of the transmitter (Table 1) and the absence or very low level of cultural noise. Nevertheless, late time gates were affected by noise in a few areas characterized by low signal. These gates were semiautomatically identified and removed by establishing another threshold in the slopes of the dB/dt transients. A slope threshold of ± 0.3 $\ln(\mathrm{dBdt})/\ln(\mathrm{time})$ was found to be characteristic of the onset of significant noise. For each recording, the earliest gate to exceed this threshold and all subsequent gates were eliminated (Figure 4). Table 3 shows the percentage of recordings for all three survey areas for which the last eight gates were removed. Except for the 7828-μs time gate of the HR1 data set, it was necessary to eliminate very few late time gates from the two high-resolution data sets; strong signals were recorded in the HR1 and HR2 data sets through to the latest one or two time gates. We had to purge significantly more late time gates from the regional survey data set (Table 3), which crossed several areas distinguished by relatively high resistivities and lower signal.

Timing and amplitude calibrations

Calibration of the time between transmitter current turn off and recording onset and calibration of the amplitudes were carried out simultaneously. The procedure involved comparing VTEM recordings to synthetic dB/dt values derived from a layered earth model based on high-quality ground-based TEM data acquired with the WalkTEM instrument (developed in-house at Aarhus University; details are in Table 4). Comparisons between VTEM measurements and values based on the WalkTEM system were made at 13 locations in the Okavango Delta, and the results were averaged. The WalkTEM instrument had been finely calibrated beforehand at a very well-understood test site in Denmark (Foged et al., 2013). Soundings with the WalkTEM system were made within 25 m of VTEM recordings and inverted for 19-layer 1D smooth models. These reference models were used to forward model VTEM responses at the elevations of the VTEM recordings. Each VTEM recording was then matched to the respective WalkTEM-based values to within a set tolerance (Figure 5). Two variables of the helicopter recording were evaluated: a time shift to add or subtract to the time of each gate and an amplitude factor by which to multiply the dB/dt value of each gate. A simple MATLAB (The MathWorks, Inc.) script was used to adjust these two variables to minimize the least-squares misfit between the WalkTEM-based and measured HTEM recordings.

Considering the regional hydrologic conditions beneath the Okavango Delta, the moderately shallow to deep resistivity structure beneath our study site very likely remained constant during the four years between the helicopter VTEM survey and the ground-based WalkTEM measurements. However, because of increased rainfall several months prior to the WalkTEM measurements, river

Table 1. Details of the Okavango Delta, Botswana, helicopter EM survey and parameters of VTEM instrument used.

Parameter	Survey area		
	Regional	HR1	HR2
Survey area size	28,000 km^2	25 km^2	35 km^2
Line spacing	2 km	50 m	50 m
Line-km recorded	14,930 km	815 km	505 km
Altimetry system	Radar mounted on underside of helicopter		
GPS system	Towed behind helicopter		
Tx pulse repetition rate	25 Hz		
Nominal current	206 A		
Pulse width	7.3434 ms		
Nominal survey speed	80 km/hr (~43 knots)		
Recording sample rate	10 samples/s		
Distance between samples along flight line	~2.5 m		
Nominal Tx/Rx height	50 m		
Tx loop diameter	26 m		
Tx loop turns	4		
Tx moment	440,000 Am^2		
Time gates (μs)	21, 31, 42, 52, 62, 73, 83, 99, 120, 141, 167, 198, 234, 281, 339, 406, 484, 573, 682, 818, 974, 1151, 1370, 1641, 1953, 2307, 2745, 3286, 3911, 4620, 5495, 6578, 7828		

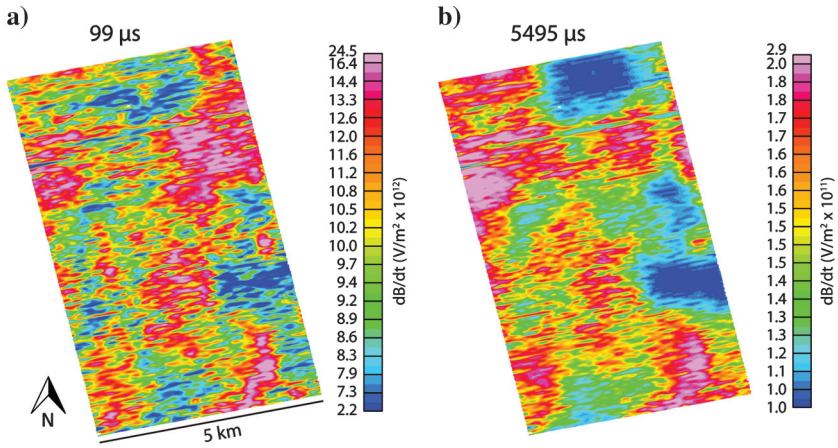

Figure 3. Map views of dB/dt for the (a) 99 and (b) 5495 μs time gates extracted from the HR2 HTEM survey. Data were acquired in a west-southwest–east-northeast direction. Artificial lineations that affect all time gates are indicative of leveling errors.

and stream channels that had not carried water in decades began to flow, such that the very shallow groundwater regime and associated resistivity structure were altered. For this reason, all time gates affected by the resistivity of the very shallow subsurface (i.e., those less than 99 μs) were omitted from the calibration procedure. Late gates were also deemed unsuitable for calibration purposes because of a significant difference in the transmitter moments of the two instruments; the lower moment WalkTEM instrument had a smaller depth of investigation than the higher moment VTEM system. The 15 gates from 99 to 1150 μs were used for the initial calibrations. They resulted in an average time shift of 29 ± 8 μs and an average amplitude factor of 1.44 ± 0.14 with a low average rms of $0.26 \pm 0.11\%$. To determine if we had eliminated a sufficient number of early gates (for near-surface variations) and late gates (for the different depth sensitivities of the two systems), the calibrations were also performed using only the seven gates from 198 to 573 μs. The results were similar, with an average time shift of 32 ± 8 μs, an average amplitude factor of 1.45 ± 0.15, and an average rms of $0.09 \pm 0.08\%$. Based on these results, we chose a time shift of 30 μs and an amplitude factor of 1.44 for the entire survey. These were applied by adding 30 μs to the center time of all time gates and multiplying all dB/dt values by 1.44.

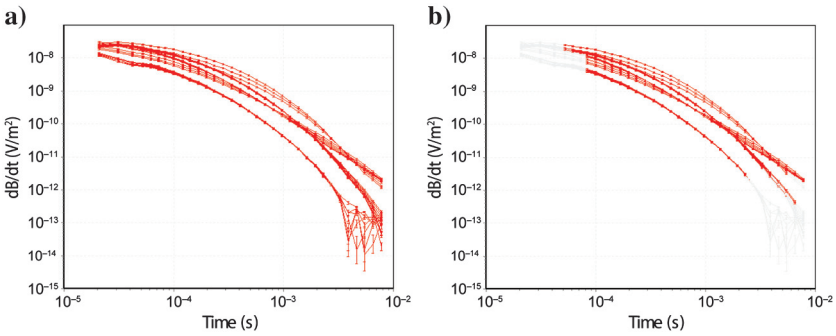

Figure 4. Editing of time gates for 25 example recordings. (a) No editing showing all 33 time gates from 21 to 7828 μs for all recordings. (b) The same recordings after gate editing. Early and late time gates were automatically evaluated for anomalous changes in dB/dt that resulted from the effects of residual transmitter current and the onset of significant noise, respectively. Once identified, the affected time gates were eliminated from the processing flow.

Effect of data processing on inversion results

After each processing step, the data were inverted for a four-layer model using a horizontally constrained inversion scheme (Auken and Christiansen, 2004). For each inversion, the starting model had a uniform resistivity of 50 Ωm and layer boundaries at 25, 70, and 150 m. By using exactly the same inversion parameters (including the starting model), any effects of inversion nonuniqueness should have been approximately the same for all resultant models.

Figure 6 shows the inversion results from a representative 5-km-long cross section based on HR2 (a) original data ($14.67 \pm 2.66\%$ rms) (b) data after editing of early and late gates ($0.65 \pm 0.30\%$ rms), and (c) data after gate editing and incorporation of data calibration ($0.51 \pm 0.39\%$ rms). Differences in the resistivities and depths of the three inversion results are highlighted by the average 1D models displayed in Figure 7, which also shows the depth to basement determined from nearby seismic refraction surveys and drilling. Data editing brings the rms misfit to an acceptable level (compare Figure 6b to Figure 6a), whereas the most significant

Table 2. Early gate editing of recordings from the three survey areas. Values indicate the percentage of each of the first eight gates that were removed.

	Early time gates removed							
Survey area	21 μs	31 μs	42 μs	52 μs	62 μs	73 μs	83 μs	99 μs
HR1	100.0%	95.4%	95.3%	89.5%	64.1%	51.6%	18.4%	7.6%
HR2	100.0%	92.7%	91.6%	82.8%	67.2%	52.8%	5.1%	1.6%
Regional	100.0%	92.8%	92.2%	77.0%	60.2%	50.6%	10.9%	5.8%

Table 3. Late gate editing of recordings from the three survey areas. Values indicate the percentage of each of the last eight gates that were removed.

	Late time gates removed							
Survey area	2307 μs	2745 μs	3286 μs	3911 μs	4620 μs	5495 μs	6578 μs	7828 μs
HR1	0.02%	0.03%	0.04%	0.04%	0.04%	0.04%	2.44%	39.67%
HR2	0.01%	0.01%	0.01%	0.02%	0.02%	0.02%	0.06%	0.50%
Regional	3.7%	4.3%	5.6%	8.7%	10.0%	10.8%	14.1%	24.6%

changes resulting from calibration are reductions in layer resistivity and shallowing of the principal layer boundaries (Figure 6c; compare the red dashed-dotted and solid blue lines in Figure 7).

Accounting for residual leveling errors and inaccuracies in altimetry through inversion

Multiple inversion strategies were tested in an attempt to produce resistivity models devoid of the artificial lineations in the original data (Figure 3). The progressive changes with each step are presented in Figure 8, which shows the second layer of a four-layer inversion of the HR2 data after editing of the time gates and application of the timing and amplitude calibration factors. The resistivity of the start models was uniformly 50 Ωm. Testing demonstrated that the start model did not have a significant effect on the inverted model.

An initial inversion of the HR2 data set for layer resistivities and depths using a pseudo-2D laterally constrained inversion scheme (Auken and Christiansen, 2004) reveals the strong influence of the lineations in the original data (Figure 8a). Constraints were made only along flight lines, such that unless otherwise necessary to fit the data, layer resistivities and depths between adjacent recordings were allowed to vary by factors of 1.2 and 1.3, respectively, using a reference distance of 25 m and a power-law dependence of 0.5. Our first attempt to minimize the effects of lineations in the original data involved applying a pseudo-3D spatially constrained inversion scheme (Viezzoli et al., 2008), which used model constraints in both lateral directions by grouping sounding points across as well as along recording lines (Figure 8b). The same resistivity and depth constraints were used along the flight lines, but their strengths between recordings on adjacent lines were reduced to 1.7 (resistivity) and 1.8 (depth) to account for the 50-m line-spacing versus the 25-m interval between the stacked recordings along the lines. Clearly, the lineations were markedly reduced by allowing recordings on neighboring lines to influence the inversion process (compare Figure 8b to 8a). The rms increased only slightly from 0.86 ± 0.89% for the quasi-2D scheme to 1.00 ± 0.70% for the quasi-3D scheme.

To remove some of the remaining lineations, the transmitter and receiver altitude was added as an inversion parameter (Figure 8c). The inverted altitudes were allowed to vary by up to 3 m from the reported altitudes and by up to a factor of 1.3 from neighboring recordings unless the data required otherwise. Although the average change between measured and inverted altitudes was only 0.003 m (changes were allowed to be either positive or negative relative to the altitude estimates provided by the contractor), indicating that the average altitude for the entire survey was correct, the mean absolute difference between the measured and inverted altitudes was 0.6 m (Figure 8c). This demonstrates that as many altitudes were overestimated by an average of 0.6 m as underestimated by the same average amount. The rms remained essentially unchanged (around 1%) with the addition of the altitude parameter. The addition of the transmitter and receiver altitude as an inversion parameter resulted in a minor reduction in the lineations and small changes to the resistivity pattern (compare Figure 8c to Figure 8b).

Table 4. Specifications of the WalkTEM ground-based TEM instrument used to make recordings for calibrating the VTEM data set. Low- and high-moment configurations are used to sample shallower and deeper depths, respectively.

	Low moment	High moment
Tx pulse repetition rate	25 Hz	25 Hz
Tx current	1 A	8 A
Tx loop size	40 × 40 m	40 × 40 m
Tx moment	1600 Am^2	12,800 Am^2
Waveform ramp-on time	125 μs	700 μs
Waveform ramp-off time	3.0E-06 μs	5.5E-06 μs
Low-pass filter	300 kHz, 450 kHz	300 kHz, 450 kHz
Time gates	34 gates between 2 and 8842 μs	34 gates between 2 and 8842 μs
Rx coil effective area	105 m^2	4200 m^2

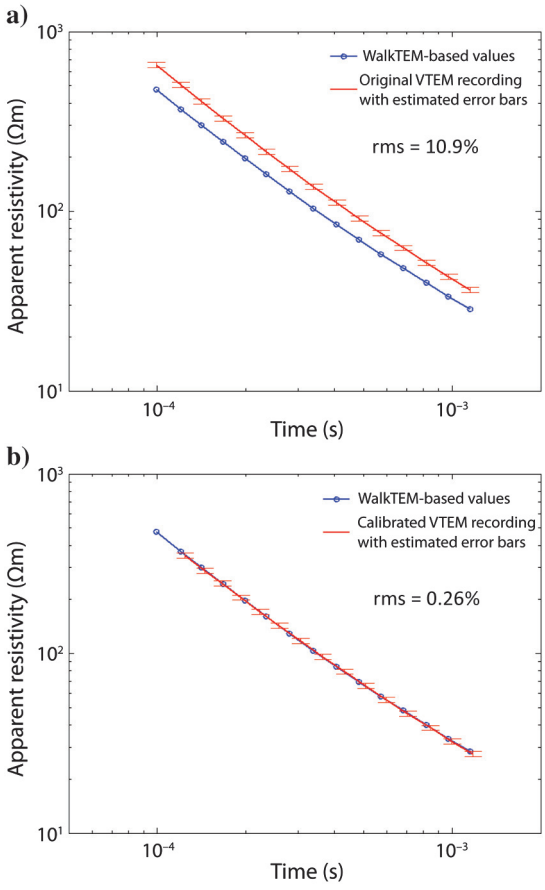

Figure 5. One example used to calibrate the VTEM recordings. Early and late gates were omitted to improve accuracy (see Figure 4 and text) (a) WalkTEM-based values and original VTEM recording. (b) WalkTEM-based values and calibrated VTEM recording. The time shift was added to all gate times. The dB/dt values were multiplied by the shift factor prior to conversion to apparent resistivities.

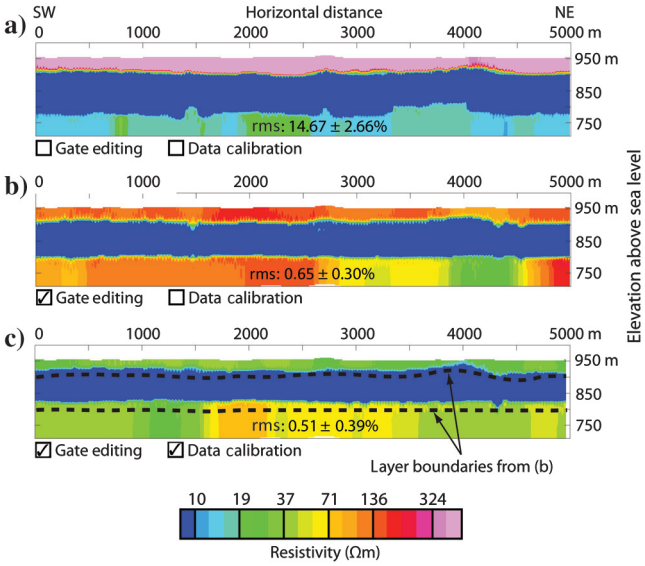

Figure 6. Inverted vertical resistivity models for line 70,200 data of survey area HR2 after application of various processing steps. "Gate editing" refers to the removal of early gates affected by residual transmitter current and the elimination of noisy late gates. "Data calibration" refers to the incorporation of a 30 μs time shift and a 1.44 multiplicative amplitude factor. The most significant changes are in the lower rms values after gate editing ($14.67 \pm 2.66\%$ versus $0.65 \pm 0.3\%$) and changes in resistivity and layer boundary depth after data calibration.

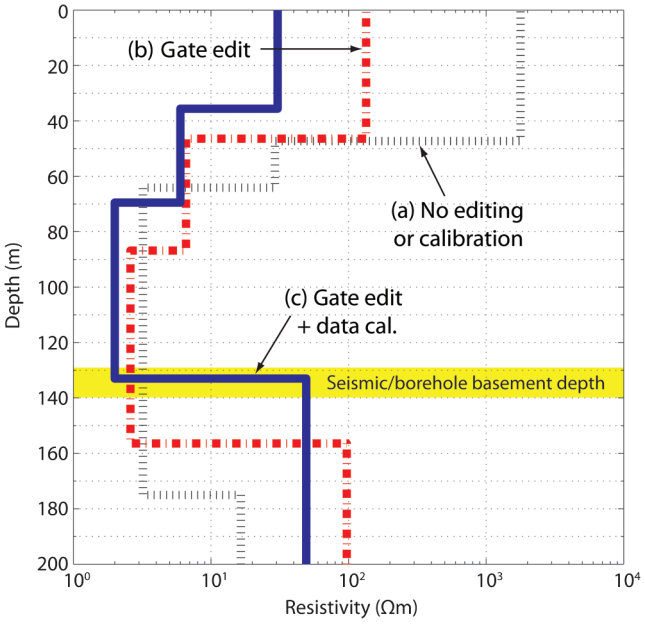

Figure 7. Average inverted resistivity models for line 70,200 data of survey area HR2 after application of various processing steps (see Figure 6). The data cannot be satisfactorily inverted without gate editing (see the high rms value in Figure 6a). The main changes after data calibration are a decrease in the resistivity of the uppermost layer and reductions in the depths to the second and third layers. The yellow overlay outlines the depths to basement determined by seismic refraction surveying and drilling at various locations within 7 to 17 km of the survey site (the basement in this area is relatively flat and horizontal).

Finally, following a suggestion of Brodie and Sambridge (2006), a line-to-line amplitude shift factor was introduced as another inversion parameter in an effort to reduce further the artificial lineations in the inversion results (Figure 8d). The amplitude shift factor was initially set to 1 and allowed to vary between 0.8 and 1.2 between the recording lines and between 0.98 and 1.02 along the lines. These ranges were chosen to keep the shift factor nearly constant along the lines while correcting leveling errors between the lines. The mean inverted shift factor for HR2 was 1.03 ± 0.05, but there were values as high as 1.12. Figure 9 shows small variations of the shift factor along the lines and larger variations between the lines. Its generally smooth character demonstrates that the shift factors did not correct for random noise. Again, the rms remained at about the same level as for the other spatially constrained inversions of Figure 8.

DISCUSSION

We have demonstrated the advantages of additional processing and inversion of VTEM data acquired across the Okavango Delta, Botswana. The popular VTEM instrument is primarily designed for mineral resource exploration (Witherly et al., 2004; Macnae, 2008) and has been only infrequently used for hydrogeologic applications (Sattel, 2009). Many of the issues we have described likely affect

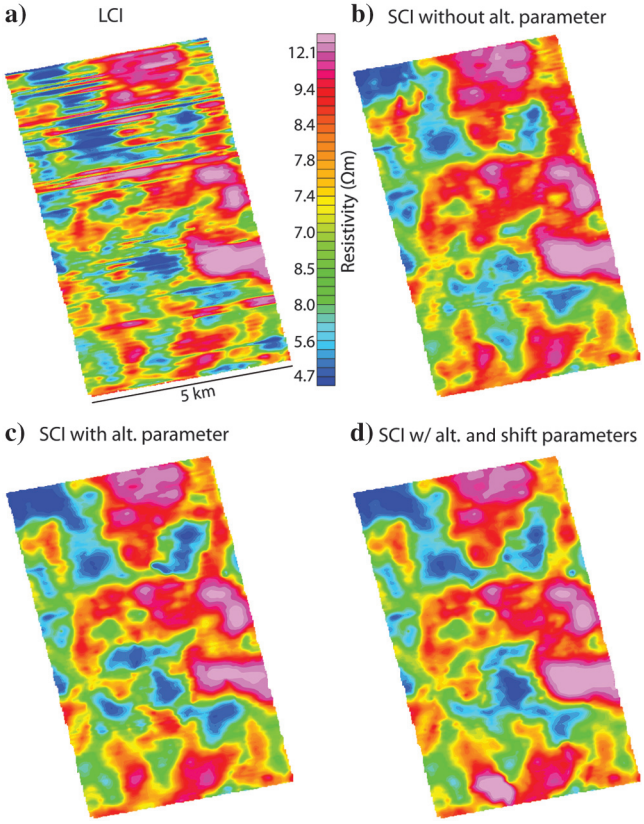

Figure 8. Comparison of layer 2 resistivities resulting from four-layer inversions of HR2 data that have been subjected to gate editing and timing and amplitude calibrations using (a) a pseudo-2D LCI scheme, (b) a pseudo-3D SCI scheme, (c) as for (b) but with transmitter and receiver altitudes included as inversion parameters, and (d) as for (c), but with a data shift inversion parameter.

other HTEM data sets collected for environmental assessments, geologic and hydrologic mapping, and the exploration of metallic ore bodies that yield weak EM anomalies. With only minor modifications, the processing and inversion strategy described in this contribution can be applied to any helicopter TEM data set. As long as ground resistivities have not changed over time, the recording of a few well-calibrated ground-based TEM data sets would allow our strategy to be applied to "historical" helicopter data sets.

The first two processing steps of time-gate editing and data calibration were required to reliably invert the data. Prior to gate editing, the HR2 data were not well modeled, as demonstrated by an rms of nearly 15% for the model in Figure 6a. Following editing, the rms was less than 1% (Figure 6b). The removal of the early gates contaminated by persistent currents in the transmitter loop was primarily responsible for the reduction in rms. Due to the varying strength of the recorded signal, the number of time gates affected by transmitter-current contamination varied from recording to recording. Our approach of selectively editing the earliest time gates made it possible to remove only those gates for which contamination negatively affected the inversion results. This allowed time gates with a sufficiently strong earth response to be retained and thus provide more near-surface information than if, for example, all gates before 99 μs would be discarded. In the HR2 survey area, relatively few recordings required the removal of the last 1–3 gates due to noise. Again, our approach of selectively removing time gates, allowed as much deep information to be retained as possible.

Timing and amplitude calibration of the HTEM data was made possible by taking advantage of accurate ground-based TEM measurements made with a finely calibrated instrument. This led to another substantial change in the inversion results (Figures 6c and 7).

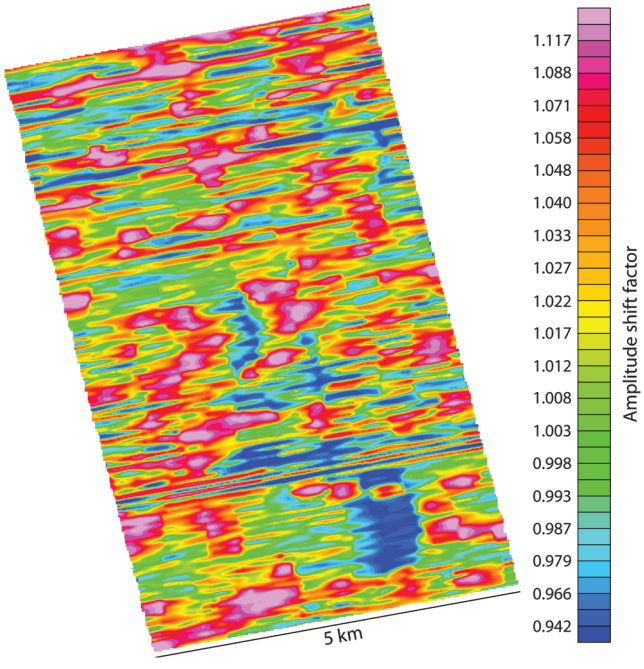

Figure 9. Inverted amplitude shift factor. This parameter was allowed to vary between 0.8 and 1.2 and by no more than 2% between neighboring recordings along a line. The lineations of the shift parameter parallel the flight lines.

The most important changes were a 77% decrease in surface-layer average resistivity and 15%–23% reductions in the depths to layer boundaries. Although the basic pattern of a thick resistive surface layer underlain successively by a thick conductive layer and a resistive half-space was common to all models, the changes in the resistivities and depths significantly affect interpretations of the models. The average 133-m depth to the resistive basement in the final model (Figures 6c and 7) closely matches 135- and 140-m basement depths determined by refraction surveying ~7 km to the north and ~17 km to the southeast of our survey site (Greenwood and Curruthers, 1973), respectively, and a 129-m basement depth observed in a borehole ~12 km to the northwest of the site (the basement in this region is approximately flat and horizontal). In contrast, the 157- and 175-m basement depths in the other two models of Figures 6 and 7 are very different from the seismic refraction and borehole basement depths.

Constant-depth resistivity maps extracted from the pseudo-2D laterally constrained inversion models derived from the gate-edited and calibrated data were contaminated by artificial lineations parallel to the flight lines (Figure 8a). These lineations were a consequence of inadequate data leveling (Figure 3). The use of the pseudo-3D spatially constrained inversion scheme markedly reduced the lineations (compare Figure 8b to Figure 8a). Although the across-line constraints of the pseudo-3D scheme brought the inverted resistivities on adjacent recording lines much closer together, some artificial lineations were still evident. In an attempt to correct this, two additional parameters were incorporated in the inversion process.

The first additional parameter was the altitude of the transmitter and receiver loops. The net change between the reported and inverted altitudes was nearly zero, but the average of the absolute changes was 0.6 m. Residual lineations were reduced somewhat as a result of this step (compare Figure 8c to Figure 8b). Including a line-to-line amplitude shift factor removed the remaining lineations by essentially fine-tuning the 1.44 amplitude factor applied to all recordings during calibration (compare Figure 8d to Figure 8c). Note how the shift-factor pattern generally follows the flight lines (Figure 9). Tests allowing the shift factor to vary outside the relatively narrow 0.8–1.2 range resulted in shift-factor patterns that started to mimic the hydrogeology rather than the flight lines (i.e., there was an inevitable trade-off between the shift factors and the resistivities and depths of the inverted models).

CONCLUSIONS

Our combined processing (including editing) and inversion strategy developed for the Okavango Delta VTEM data is quite general. After accounting for different data formats, it could be applied to any HTEM data set, including those recorded many years ago. Two principal issues are addressed. The first is to edit and calibrate the data, such that they could be successfully inverted to produce plausible models (i.e., models that fit the data with low rms values). The second is to fine-tune the inversion process to remove lineations that result from leveling problems in the original data.

The editing of time gates was carried out in a semiautomated fashion by establishing thresholds in dB/dt–t slope changes between consecutive time gates. Early and late gates were evaluated for transmitter-current contamination and noise, respectively. Nearly all 21–52-μs time gates were removed, and a smaller but significant number of 62–99-μs gates were discarded. In contrast, very few late

time gates from the HR1 and HR2 data sets were eliminated because of low S/N. A somewhat larger percentage of late time gates was eliminated from the regional data set, which sampled some areas with more resistive ground that produced lower recorded signals at late times.

The data were calibrated by applying a +30-μs time shift and a multiplicative 1.44 amplitude correction factor to all gates. These values were determined by comparing a suite of VTEM recordings with coincident reference HTEM recordings effectively estimated from 13 ground-based TEM measurements made with an accurately calibrated instrument. The calibration resulted in significant changes to the inverted models. The average basement depth in the model derived from the gate-corrected and calibrated data set closely matched the regional basement depth determined from seismic refraction surveying and drilling, whereas the average basement depths from the other two models were much too deep. We suggest that data calibration is a crucial step in the processing of HTEM data.

After gate editing and calibration, the data were ready for inversion. Unfortunately, artificial lineations in the original data set resulted in similar features being generated in the initial pseudo-2D laterally constrained inversion models. These lineations were substantially reduced after applying a pseudo-3D spatially constrained inversion scheme. Nevertheless, faint lineations continued to be seen in the inversion models. The remnant lineations were effectively removed after adding transmitter and receiver altitude and a line-to-line amplitude shift factor to the list of inverted parameters. The benefit of this method over microleveling and directional filtering is that it corrects known problems with the HTEM data sets themselves rather than arbitrarily filtering the models to produce smoothed final results.

ACKNOWLEDGMENTS

We thank the four journal reviewers for their constructive comments on an earlier version of this manuscript. We also thank the Swiss National Science Foundation for funding this work, the Botswana Department of the Geological Survey (DGS) for access to the Okavango Delta helicopter TEM data sets, and P. Gazoty for patiently implementing numerous changes to the processing schemes of the Aarhus Workbench.

REFERENCES

Auken, E., and A. V. Christiansen, 2004, Layered and laterally constrained 2D inversion of resistivity data: Geophysics, **69**, 752–761, doi: 10.1190/1.1759461.

Auken, E., L. Pellerin, N. B. Christensen, and K. Sørensen, 2006, A survey of current trends in near-surface electrical and electromagnetic methods: Geophysics, **71**, no. 5, G249–G260, doi: 10.1190/1.2335575.

Auken, E., S. Violette, N. d'Ozouville, B. Deffontaines, K. I. Sørensen, A. Viezzoli, and G. de Marsily, 2009, An integrated study of the hydrogeology of volcanic islands using helicopter borne transient electromagnetic: Application in the Galápagos Archipelago: Comptes Rendus Geosciences, **341**, 899–907, doi: 10.1016/j.crte.2009.07.006.

Beamish, D., 2002, An assessment of inversion methods for AEM data applied to environmental studies: Journal of Applied Geophysics, **51**, 75–96, doi: 10.1016/S0926-9851(02)00213-6.

Beamish, D., 2005, An airborne EM survey of a landfill that leaked: First Break, **23**, 55–60.

Beamish, D., and M. Young, 2009, Geophysics of Northern Ireland: The Tellus effect: First Break, **27**, 43–49.

Best, M. E., V. M. Levson, T. Ferbey, and D. McConnell, 2006, Airborne electromagnetic mapping for buried quaternary sands and gravels in northeast British Columbia, Canada: Journal of Environmental and Engineering Geophysics, **11**, 17–26, doi: 10.2113/JEEG11.1.17.

Brodie, R., and R. Lane, 2003, The importance of accurate altimetry in AEM surveys for land management: Exploration Geophysics, **34**, 77–81, doi: 10.1071/EG03077.

Brodie, R. S., and M. Sambridge, 2006, A holistic approach to inversion of frequency domain airborne EM data: Geophysics, **71**, no. 6, G301–G312, doi: 10.1190/1.2356112.

Christiansen, A. V., E. Auken, and K. Sørensen, 2009, The transient electromagnetic method, *in* R. Kirsch, ed., Groundwater geophysics: Springer, 179–226.

Christiansen, A. V., E. Auken, and A. Viezzoli, 2011, Quantification of modeling errors in airborne TEM caused by inaccurate system description: Geophysics, **76**, no. 1, F43–F52, doi: 10.1190/1.3511354.

Cox, L. H., G. A. Wilson, and M. S. Zhdanov, 2012, 3D inversion of airborne electromagnetic data: Geophysics, **77**, no. 4, WB59–WB69, doi: 10.1190/geo2011-0370.1.

Davis, A. C., and J. Macnae, 2008, Quantifying AEM system characteristics using a ground loop: Geophysics, **73**, no. 4, F179–F188, doi: 10.1190/1.2943189.

Eberle, D., and B. Siemon, 2006, Identification of buried valleys using the BGR helicopter-borne geophysical system: Near Surface Geophysics, **4**, 125–133, doi: 10.3997/1873-0604.2005038.

Foged, N., E. Auken, A. Christiansen, and K. I. Sørensen, 2013, Test site calibration and validation of airborne and ground based TEM systems: Geophysics, **78**, no 2, E95–E106, doi: 10.1190/geo2012-0244.1.

Fountain, D., R. Smith, T. Payne, and J. Lemieux, 2005, A helicopter time-domain EM system applied to mineral exploration: System and data: First Break, **23**, 73–78.

Greenwood, P. G., and R. M. Carruthers, 1973, Geophysical surveys in the Okavango Delta, Botswana: Institute of Geological Sciences Geophysics Division, Report 15, 23.

Jørgensen, F., W. Scheer, S. Thomsen, T. O. Sonnenborg, K. Hinsby, H. Wiederhold, C. Schamper, T. Burschil, B. Roth, R. Kirsch, and E. Auken, 2012, Transboundary geophysical mapping of geological elements and salinity distribution critical for the assessment of future sea water intrusion in response to sea level rise: Hydrolology and Earth System Sciences Discussions, **9**, 2629–2674, doi: 10.5194/hessd-9-2629-2012.

Kirkegaard, C., T. O. Sonnenborg, E. Auken, and F. Jorgensen, 2011, Salinity distribution in heterogeneous coastal aquifers mapped by airborne electromagnetics: Vadose Zone Journal, **10**, 125–135, doi: 10.2136/vzj2010.0038.

Macnae, J., 2008, Airborne EM systems compared: Preview, **133**, April Issue, 24–29, doi: 10.1071/PVv2008n133.

Macnae, J., and S. Baron-Hay, 2010, Reprocessing strategy to obtain quantitative early time data from historic VTEM surveys: ASEG Extended Abstracts, **1**, 1–4, doi: 10.1071/ASEG2010ab050.

Macnae, J. C., R. Smith, B. D. Polzer, Y. Lamontagne, and P. S. Klinkert, 1991, Conductivity-depth imaging of airborne electromagnetic step-response data: Geophysics, **56**, 102–114, doi: 10.1190/1.1442945.

Nabighian, M. N., and J. C. Macnae, 1991, Time domain electromagnetic prospecting methods, *in* M. N. Nabighian, ed., Electromagnetic methods in applied geophysics, vol. 2, Application, parts A and B: SEG Investigations in Geophysics 3, 427–520.

Palacky, G. J., and G. F. West, 1991, Airborne electromagnetic methods, *in* M. N. Nabighian, ed., Electromagnetic methods in applied geophysics, vol. 2, Application, parts A and B: SEG Investigations in Geophysics 3, 811–877.

Sattel, D., 2005, Inverting airborne electromagnetic (AEM) data with Zohdy's method: Geophysics, **70**, no. 4, G77–G85, doi: 10.1190/1.1990217.

Sattel, D., 2009, An overview of helicopter time-domain systems: ASEG Extended Abstracts, **1**, 1–6, doi: 10.1071/ASEG2009ab049.

Siemon, B., A. Christiansen, and E. Auken, 2009, A review of helicopter-borne electromagnetic methods for groundwater exploration: Near Surface Geophysics, **7**, 629–646, doi: 10.3997/1873-0604.2009043.

Siemon, B., A. Steuer, U. Meyer, and H.-J. Rehli, 2007, HELP ACEH — A post-tsunami helicopter-borne groundwater project along the coasts of Aceh, northern Sumatra: Near Surface Geophysics, **5**, 231–240, doi: 10.3997/1873-0604.2007005.

Siemon, B., A. Steuer, A. Ullmann, M. Vasterling, and W. Voß, 2011, Application of frequency-domain helicopter-borne electromagnetic for groundwater exploration in urban areas: Physics and Chemistry of the Earth, **36**, 1373–1385, doi: 10.1016/j.pce.2011.02.006.

Sørensen, K., and E. Auken, 2004, SkyTEM — A new high-resolution helicopter transient electromagnetic system: Exploration Geophysics, **35**, 191–199, doi: 10.1071/EG04194.

Steuer, A., B. Siemon, and E. Auken, 2009, A comparison of helicopter-borne electromagnetic in frequency- and time-domain at the Cuxhaven valley in Northern Germany: Journal of Applied Geophysics, **67**, 194–205, doi: 10.1016/j.jappgeo.2007.07.001.

Viezzoli, A., A. V. Christiansen, E. Auken, and K. Sørensen, 2008, Quasi-3D modeling of airborne TEM data by spatially constrained inversion: Geophysics, **73**, no. 3, F105–F113, doi: 10.1190/1.2895521.

Witherly, K., R. Irvine, and E. Morrison, 2004, The Geotech VTEM time domain helicopter EM system: 74th Annual International Meeting, SEG, Expanded Abstracts, 1–4.
Wynn, J., M. Bultman, and J. Lemieux, 2005, Airborne geophysics versus groundwater — An example, *in* D. K. Butler, ed., Near-surface geophysics, Applications and case histories, Part 2: SEG Investigations in Geophysics 13, 635–641.
Yang, D., and D. W. Oldenburg, 2012, Three-dimensional inversion of airborne time-domain electromagnetic data with applications to a porphyry deposit: Geophysics, **77**, no. 2, B23–B34, doi: 10.1190/geo2011-0194.1.